Effect of attenuation model on iodine quantification in contrast-enhanced breast CT

Mikhail Mikerov[a], Koen Michielsen[a], James G. Nagy[b], and Ioannis Sechopoulos[a, c, d]

[a]Dept. of Medical Imaging, Radboudumc, Nijmegen, The Netherlands
[b]Dept. of Mathematics, Emory University, Atlanta, GA, USA
[c]Dutch Expert Center for Screening (LRCB), Nijmegen, The Netherlands
[d]Technical Medicine Centre, University of Twente, Enschede, The Netherlands

ABSTRACT

Accurate models of the x-ray attenuation process are required for quantitative estimation of iodine concentration with model-based reconstruction methods. The choice of model is influenced not only by the accuracy sought but also by the increasing complexity when more free parameters need to be reconstructed. The applicability of three attenuation models was investigated in a single pixel problem using either two or three monochromatic beams near the K-edge energy of iodine.

We found that an empirical model with 5 components, proposed by Midgley, leads to the lowest error when modeling iodine free materials and small error in estimating iodine concentration (0.1% and 3.39%), whereas the decomposition into contributions due to photoelectric effect and incoherent scatter results in more accurate estimation of the iodine concentration (0.72%) but has larger error (8.9%) when reconstructing iodine free materials. Decomposition into base materials shows the worst results on both objectives (8.9% and 62%).

1. INTRODUCTION

Tumor characterization through quantitative functional imaging may allow for better treatment decisions in patients with breast cancer.[1] Dynamic contrast-enhanced breast CT is a new imaging modality being developed with aim to provide such functional information at good spatial and temporal resolutions. However, to maximize its clinical potential, accurate estimation of iodine concentration in the breast CT images is crucial. Current knowledge based on body CT imaging and computer simulations of contrast-enhanced breast CT indicate that the iodine concentration in the areas of interest, especially the tumor, can be expected to be in the range of 0.5 to 3.5 mg I per mL blood.[2] Coupled with sparse projections of typical breast CT systems and low photon energies that are required to increase the contrast (typically around 30 keV), the estimation of iodine concentration is a challenging task. In our implementation of contrast-enhanced breast CT, to save acquisition time and dose to the patient, individual projections are acquired only once with one of the x-ray spectra being used. This makes the use of decomposition methods in the projection domain not applicable.

Model-based methods are well suited to solve this reconstruction problem since they can use all available information about the acquisition, such as system geometry, utilized spectra, and physics models of attenuation processes. The latter determines, among other things, the number of free parameters that need to be estimated. Accurate modeling of the attenuation process is more difficult at low photon energies, where, in addition to photoelectric effect and incoherent scatter, coherent scatter also plays a role. Various parameterization schemes with different amounts of free parameters have been proposed to model attenuation.

In this work, we present the results of two experiments in which we examine the performance of three different parameterization schemes for energy dependent linear attenuation coefficients in a single pixel reconstruction problem. We focus on biological materials in the breast at x-ray energies below 49 keV and on accuracy of contrast quantification after adding iodine in the attenuation models, so we can determine which parameterization is most suitable to extend for our application, and include in our reconstruction method for quantitative breast CT imaging.

Send correspondence to Mikhail Mikerov (mikhail.mikerov@radboudumc.nl)

2. METHODS

To avoid confounding influences, we focus on estimation of the energy dependent linear attenuation coefficient between 10 keV and 49 keV in a single pixel with monochromatic beams in dual and triple energy systems. Therefore, we are not solving the geometric aspect of the CT reconstruction problem, but are rather showing the adequacy of possible models of the energy dependency of linear attenuation.

2.1 Forward model

All values in the projection domain are obtained using the Beer-Lambert law:

$$p_E = I_0 \exp\left(-L \cdot \mu_E\right), \tag{1}$$

where μ_E is the linear attenuation coefficient at energy E, I_0 is the signal before attenuation, and L is the intersection length of the ray with the pixel of interest. The values of I_0 and L were set to 1 for all experiments.

2.2 Solution of linear systems

Limiting the estimation of the linear attenuation coefficient to a single pixel allows us to solve the linear system $A\mathbf{x} = \mathbf{b}$ using two analytical methods. The first is non-negative least squares, which is applied when the linear system has either full rank or is overdetermined.[3] We solve underdetermined systems of equations using the conjugate gradient method,[3] an iterative method that requires a good initial guess. It can be shown that for underdetemined systems of equations, conjugate gradient methods applied to $A^T A\mathbf{x} = A^T\mathbf{b}$, such as CGLS and LSQR, will converge to the minimum norm solution $A^T(AA^T)^{-1}\mathbf{b}$, making their application feasible.[3]

2.3 Models of attenuation

We consider three different models for the energy dependent attenuation. The first model consists of a decomposition into base materials. In breast imaging, decomposition into adipose, fibro-glandular, and iodine components is the most evident choice. The system of equations for the single pixel problem in dual energy systems then takes the following form:

$$-\begin{pmatrix} \mu_a^L & \mu_g^L & \mu_i^L \\ \mu_a^H & \mu_g^H & \mu_i^H \\ -1 & -1 & -1 \end{pmatrix} \begin{pmatrix} f_a \\ f_g \\ f_i \end{pmatrix} = \begin{pmatrix} \ln p_L \\ \ln p_H \\ 1 \end{pmatrix} \tag{2}$$

The subscripts L and H refer to low and high energies. The last row puts a constraint on the otherwise underdetermined system of equations by enforcing conservation of volume, possibly causing undesirable behavior when the selected base materials are suboptimal to represent all expected tissues. When more than two spectra are used to acquire the images, additional rows can be added, making this system overdetermined.

The second model makes use of the physical processes underlying the attenuation of x rays. It decomposes the attenuation profile into contributions due to photoelectric effect and incoherent scatter. The energy dependency of the photoelectric effect is usually modeled using the power law

$$\Phi\left(E\right) = 1/E^3, \tag{3}$$

where E is the x-ray energy, whereas the Klein-Nishina equation is employed to describe incoherent (Compton) scatter

$$\begin{aligned} \Theta\left(E\right) = & \frac{(1+\alpha)}{\alpha^2}\left(\frac{2\left(1+\alpha\right)}{1+2\alpha} - \frac{\ln\left(1+2\alpha\right)}{\alpha}\right) \\ & + \frac{\ln\left(1+2\alpha\right)}{2\alpha} - \frac{1+3\alpha}{\left(1+2\alpha\right)^2}, \end{aligned} \tag{4}$$
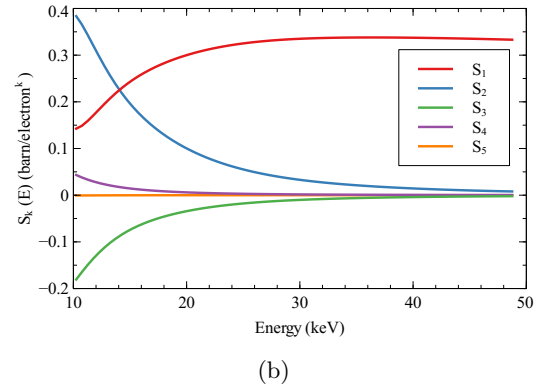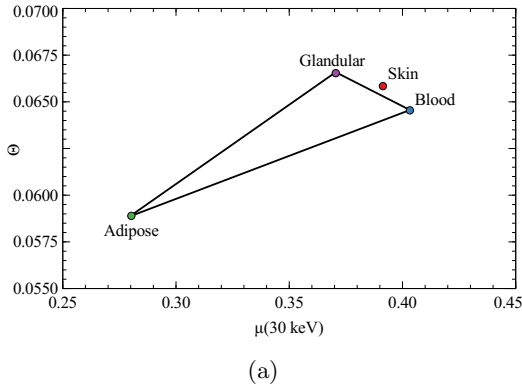
Figure 1: (a) Fitted contribution due to incoherent scatter as function of linear attenuation coefficient at 30 keV for materials present in the breast. (b) The S-parameters were calculated using compositions of materials found in the breast.

where $\alpha = E/511$ keV. However, this parameterization cannot model K-edges. Thus, in order to use this model to estimate the concentration of contrast agents, the attenuation characteristics of iodine must be included in the model. Consequently, the linear system of equations becomes:

$$-\begin{pmatrix} \phi^L & \Theta^L & \mu_{iodine}^L \\ \phi^M & \Theta^M & \mu_{iodine}^M \\ \phi^H & \Theta^H & \mu_{iodine}^H \end{pmatrix} \begin{pmatrix} f_\phi \\ f_\Theta \\ f_i \end{pmatrix} = \begin{pmatrix} \ln p_L \\ \ln p_M \\ \ln p_H \end{pmatrix},$$ (5)

meaning that measurements at three different energies are required for the linear system to have full rank.

This model can be used in dual-energy setups following the method that was proposed by Depypere et al.[4, 5] If one can write ϕ and Θ as piece-wise linear functions of some parameter, e.g., the attenuation coefficient at a given energy, only two different measurements are needed. Hence, two parameters — the attenuation coefficient at a fixed energy and the iodine volume fraction — can be reconstructed using dual-energy setups. The difficulty of applying this method for breast imaging is that it is not possible to write the attenuation coefficient as a piece-wise linear function, as indicated in figure 1a. Blood, skin, adipose and glandular tissues have very similar properties. Since any possible combination of materials in the triangle adipose-glandular-blood is theoretically possible, a systematic error is introduced as soon as the background tissue does not lie on the chosen line.

The third parameterization we included in our experiment was proposed by Midgley.[6] It decomposes the linear attenuation coefficient into energy-dependent S-parameters that are weighted by composition-dependent a-parameters:

$$\mu_E = \sum_{k=1}^{5} a_k S_k.$$ (6)

The number of S-parameters is not fixed and more parameters will lead to more accurate models. However, five S-parameters are sufficient to keep the maximum error below 2% in the energy range up to 50 keV.[6] Moreover, following that $a_{k+1} \geq a_k$, μ_E monotonically decreases with energy. The S-parameters for biological tissues in breast imaging are shown in figure 1b. They were calculated by taking into account that a-parameters are functions of atomic number and electron density. Thus, the S-parameters are obtained by solving a least-squares problem,[7] in our instance for elements that are found in breast tissues, specifically H, B, C, N, O, Na, Al, Si, P, S, Cl, Ar, K, Ca and Fe. As with the previous model, this parameterization scheme cannot account for K-edges. Thus, we extended this model to include the attenuation coefficient of iodine

$$\mu_E = \sum_{k=1}^{5} a_k S_k (1 - f) + f \mu_{iodine}.$$ (7)

Assuming that the iodine volume fraction f is very small, the resulting system of equations in a dual-energy setup can be written as

$$-\begin{pmatrix} S_1^L & S_2^L & S_3^L & S_4^L & S_5^L & \mu_{iodine}^L \\ S_1^H & S_2^H & S_3^H & S_4^H & S_5^H & \mu_{iodine}^H \end{pmatrix} \begin{pmatrix} a_1 \\ a_2 \\ a_3 \\ a_4 \\ a_5 \\ f \end{pmatrix} = \begin{pmatrix} \ln p_L \\ \ln p_H \end{pmatrix}. \tag{8}$$

2.4 Experiments

We examine the effect of the attenuation model on the accuracy of skin and iodine reconstruction in dual- and triple-energy acquisitions. We use skin as a good example of a background material that needs to be modeled correctly in order to avoid systematic errors that will otherwise propagate into the estimated iodine concentration in model-based reconstruction. Since model-based reconstruction tries to minimize the mismatch in the projection domain, incorrect linear attenuation coefficients in background material must be compensated by adjusting iodine concentration, which leads to lower accuracy.

The tissue background for the experiment including iodine contrast consists of a mixture of 50% adipose tissue, 50% fibro-glandular tissue; the volume fraction of blood is 30%. Varying amounts of iodine (0–20 mg/mL) were then added to the blood fraction. Our contrast agent is modeled as pure iodine. We assume that the attenuation of the contrast agent suspension medium is equal to that of blood. All materials were modeled with corresponding tissue substitutes.[8–10] and the attenuation profiles of elements were obtained from XrayDB.[11]

The energies of the low and high energy spectra in the dual-energy setup were set to 30 keV and 34 keV, and the third energy for the triple-energy setup was set to 38 keV. Water was used as initialization for Midgley's parameterization. No initialization was needed for the other models since the resulting systems of equations were not underdetermined. The decomposition into photoelectric effect and incoherent scatter was considered only in the triple-energy setting.

# 3. RESULTS

3.1 Reconstruction of skin

Figure 2a shows the relative error of the reconstructed attenuation coefficient of skin with three methods. The largest deviation (8.9% at 10 keV and $1.44 \cdot 10^{-4}$ volume fraction of iodine) results from the model that decomposes the background into adipose and glandular tissues. The most accurate result is achieved with Midgley's model in a triple-energy setup (0.1% at 10 keV and $-2.27 \cdot 10^{-6}$ volume fraction of iodine). Complete results are shown in table 1.

Table 1: Mean and maximum absolute relative errors on attenuation between 10 keV and 49 keV, and reconstructed iodine volume fraction for skin.

attenuation model	mean error	maximum error	iodine volume fraction
PE + Compton (double)	0.71%	4.95%	0.00
Base materials (double)	3.50%	8.88%	$1.44 \cdot 10^{-4}$
Base materials (triple)	3.50%	9.28%	$1.14 \cdot 10^{-4}$
Midgley (double)	1.13%	2.25%	$-3.80 \cdot 10^{-5}$
Midgley (triple)	0.07%	0.18%	$-2.27 \cdot 10^{-6}$
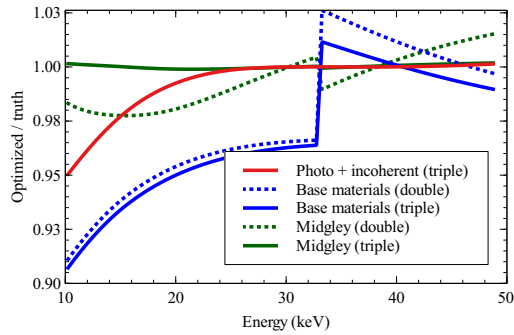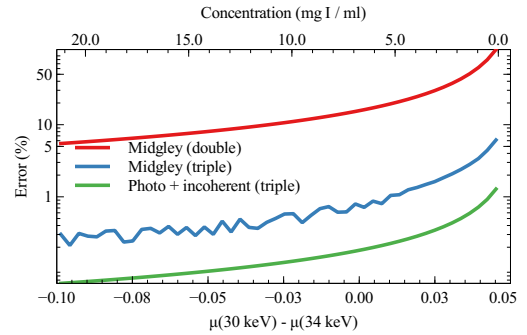
Figure 2: (a) Proportional error between reconstructed and true linear attenuation coefficient of skin when using different models of attenuation and number of spectra. (b) Error in estimated iodine concentration as function of the difference between the linear attenuation of the mixture below and above the K-edge of iodine and concentration in blood. The negative region indicates rise in the attenuation due to K-edge. The background tissue was 50% adipose and 50% fibro-glandular tissues; volume fraction of blood was 30%.

3.2 Estimation of iodine concentration

Figure 2b shows the error in iodine concentration estimation as a function of the difference between linear attenuation at 30 keV and 34 keV, resulting from the iodine K-edge when reconstructed using Midgley's model in dual- and triple-energy setups. The corresponding concentration of iodine is shown on top. The error is 62% and 3.39% at 0.97 mg I per mL of blood with double-energy and triple-energy setups, respectively. An even lower error (0.72%) is achieved with the decomposition into photoelectric effect and incoherent scatter with monochromatic radiation.

4. DISCUSSION

The aim of this study was to find the most accurate parameterization scheme for model-based reconstructions methods for breast CT with a focus on quantitative accuracy of the estimation of iodine concentration. Unsurprisingly, the base material decomposition into iodine, adipose and glandular tissues is the least accurate method to reconstruct skin. The error is substantial as it clearly shows that the iodine concentration in skin will not be zero. The accuracy improves only slightly when using a triple-energy system.

Decomposition into contributions due to photoelectric effect and incoherent scatter on the other hand, is very accurate above 25 keV. However, its accuracy drops noticeably in the lower energy range. This can be explained by the contribution due to coherent scatter in this low-energy range, which is absent from this model.

Finally, Midgley's parameterization in the triple-energy setup leads to the most accurate results for skin. The parameterization with three energies achieves better results than the one with two. In particular, triple energy optimization has negligible iodine signal in skin even though the linear system remains underdetermined. This is most likely explained by our initialization which assigns a good approximation of the relative contributions of the scatter processes. Parameters not well constrained in the problem would then not end up far from a reasonable value. Further examination of how the initialization with water holds up for calcifications will give an indication on the limitations of using a simple homogeneous initialization in patient images.

Our experiment shows that the decomposition into contributions due to photoloelectric effect and incoherent scatter is equally good as Midgley's parameterization at energies above 25 keV. However, the result shown in figure 2a represents the ideal case. Introduction of real polychromatic spectra will complicate the situation. Besides, one of the spectra must have mean average energy below the K-edge of iodine to capture it, which leads to nonzero fluence in the low energy range. Taking into account that the attenuation coefficients are highest in this range, it is favorable to avoid systematic errors that are introduced due to less accurate models when using model-based reconstruction methods. Nevertheless, the mono-energetic simplification is the main limitation of this study that needs to be addressed.

The triple-energy system leads to better results in the relevant concentration range in our application, i.e., below 3.5 mg I per mL blood. Notably, it is not enough to just have beam energies on either side of the K-edge. Accurate quantification requires the K-edge that causes an increase in attenuation at relevant energies, otherwise, the accuracy quickly decreases when the K-edge is not causing such increase as can be observed in figure 2b. Since any allowed combinations of S-parameters are monotonically decreasing functions, the K-edge does not need to be modeled in order to connect the points on the linear attenuation profile at relevant energies. The continuous decrease in accuracy can be explained by different slopes of iodine before and after the K-edge, which means that there is still some information about iodine content present. The situation changes when the measurement at the third energy is added. Now, the only way to account for rise in attenuation and different slopes below and above the K-edge is to add the correct fraction of iodine.

5. CONCLUSION AND OUTLOOK

In this simplified numerical study we have shown that the attenuation model influences accuracy of iodine reconstruction in contrast-enhanced breast CT at energies below 49 keV. Such models could lead to underdetermined linear systems. Nevertheless, an accurate solution can be found if triple-energy systems and appropriate initialization are used. In our future research, we will examine if these conclusions remain valid for polychromatic spectra before incorporating the preferred attenuation model in our model-based reconstruction for breast CT.

Acknowledgment

REFERENCES

[1] J. Wu, G. Cao, X. Sun, J. Lee, D. L. Rubin, S. Napel, A. W. Kurian, B. L. Daniel, and R. Li, "Intratumoral spatial heterogeneity at perfusion mr imaging predicts recurrence-free survival in locally advanced breast cancer treated with neoadjuvant chemotherapy," *Radiology*, vol. 288, no. 1, pp. 26–35, 2018, pMID: 29714680. [Online]. Available: https://doi.org/10.1148/radiol.2018172462

[2] M. Caballo, R. Mann, and I. Sechopoulos, "Patient-based 4D digital breast phantom for perfusion contrast-enhanced breast CT imaging," *Medical Physics*, vol. 45, no. 10, pp. 4448–4460, Oct. 2018. [Online]. Available: https://onlinelibrary.wiley.com/doi/10.1002/mp.13156

[3] Å. Björck, *Numerical Methods for Least Squares Problems*. SIAM, 1996.

[4] M. Depypere, J. Nuyts, N. van Gastel, G. Carmeliet, F. Maes, and P. Suetens, "An iterative dual energy CT reconstruction method for a K-edge contrast material," N. J. Pelc, E. Samei, and R. M. Nishikawa, Eds., Lake Buena Vista, Florida, Mar. 2011, p. 79610M. [Online]. Available: https://doi.org/10.1117/12.878162

[5] B. De Man, J. Nuyts, P. Dupont, G. Marchal, and P. Suetens, "An iterative maximum-likelihood polychromatic algorithm for CT," *IEEE Transactions on Medical Imaging*, vol. 20, no. 10, pp. 999–1008, Oct. 2001. [Online]. Available: http://ieeexplore.ieee.org/document/959297/

[6] S. M. Midgley, "A parameterization scheme for the x-ray linear attenuation coefficient and energy absorption coefficient," *Physics in Medicine and Biology*, vol. 49, no. 2, pp. 307–325, Jan. 2004. [Online]. Available: https://iopscience.iop.org/article/10.1088/0031-9155/49/2/009

[7] ——, "A method for estimating radiation interaction coefficients for tissues from single energy CT," *Physics in Medicine and Biology*, vol. 59, no. 23, pp. 7479–7499, Dec. 2014. [Online]. Available: https://iopscience.iop.org/article/10.1088/0031-9155/59/23/7479

[8] "ICRP, 2009. Adult Reference Computational Phantoms. ICRP Publication 110. Ann. ICRP 39 (2)."

[9] D. R. White, J. Booz, R. V. Griffith, J. J. Spokas, and I. J. Wilson, "Report 44," *Journal of the International Commission on Radiation Units and Measurements*, vol. os23, no. 1, pp. NP–NP, 04 2016. [Online]. Available: https://doi.org/10.1093/jicru/os23.1.Report44

[10] J. W. Byng, J. G. Mainprize, and M. J. Yaffe, "X-ray characterization of breast phantom materials," *Physics in Medicine and Biology*, vol. 43, no. 5, pp. 1367–1377, may 1998. [Online]. Available: https://doi.org/10.1088/0031-9155/43/5/026

[11] "Xraydb," https://github.com/xraypy/XrayDB.